LFER and 3D-QSAR Analysis of Febrifugine Derivatives against *Plasmodium falciparum* FCR-3 Strain

Nur Aina, Tegar Achsendo Yuniarta*, Dini Kesuma

Faculty of Pharmacy, University of Surabaya, Kalirungkut, Surabaya 60293, Indonesia
**Corresponding author. Email: tegar.achsendo@staff.ubaya.ac.id*

ABSTRACT
Malaria is a serious disease caused by Plasmodium through the bite of the female Anopheles mosquito. Due to resistance to artemisin, a first-line antimalarial, new compounds are needed. This study aims to obtain a QSAR model from febrifugine derivatives against the *Plasmodium falciparum* FCR-3 strain. 3D-QSAR modelling using Cloud-3D QSAR, and LFER (Linear Free Energy Relationship) Hansch QSAR equation using DTC QSAR have been carried out in this study. The results showed that the best 3D-QSAR model indicating the addition of steric substituents on C6 and C7 of quinazolinone, C4 and C5 of piperidine, and electronic substituents on C5 might increase activity. Furthermore, the best LFER Hansch QSAR equation is shown by pIC50 = 0,069(±0,0009) $(logP)^2$ +3,5234(±0,0461) (n = 40 R^2 = 0.9938; Q^2 LOO = 0.9926; R_m^2 average = 0.9895; R^2-Q^2 LOO = 0.0012; ΔR_m^2 = 0.0037; Q^2 F1 = 0.9956; Q^2 F2 = 0.9955; CCC = 0.9978). Based on the LFER Hansch QSAR equation, the physicochemical parameter which must be considered to increase the activity is the lipophilic parameter. In addition, febrifugine and its derivatives are predicted to possess a good ADMET profile. The results of this QSAR model can be used to develop further antimalarials.

Keywords: QSAR, *Febrifugine, Antimalaria, FCR-3 strain*

1. INTRODUCTION

Malaria is one of the deadliest diseases caused by *Plasmodium falciparum* infection transmitted via the Anopheles female mosquito [1]. WHO has recommended Artemisinin-Based Combination Therapy as the first-line therapy in malaria treatment [2]. However, several cases of parasite resistance [3] point out the necessity for improvement in dealing with malaria, one of which is *via* drug discovery.

Febrifugine is a quinazolinone-type alkaloid isolated from Dichroa febrifuga [4], which has long been known as an antimalarial agent in Traditional Chinese Medicine [5,6]. However, it also possesses significant side effects, such as nausea, vomiting, and hepatotoxicity. Febrifugine inhibits *Plasmodium falciparum* prolyl-tRNA synthetase, which has been proven an antimalarial target [7]. It inhibits this enzyme by occupying active pockets of proline and the 3' end of tRNA [7,8].

Various derivates of febrifugine have been synthesized and have their potencies evaluated to obtain the most potent analog with low to minimal side effects [9-13]. This study created a QSAR model using the three-dimensional and LFER Hansch approach. The outcome is to obtain the most suitable correlation model, which can guide the design of novel febrifugin analogs with significant improvement in antimalarial activity. In addition, the ADMET profile of febrifugin and its derivatives have been characterized *in silico* to understand their pharmacokinetics characteristic better.

2. MATERIALS & METHODS

2.1. Dataset Preparation

This study focused on the QSAR model between febrifugine derivatives and their activity against the FCR-3 cell line. A literature study shows sixty molecules have been tested against this cell line, 10 of which do not yield specific IC50 value [9-13]. Therefore, 50 compounds will

J. Sukweenadhi and F. Setiawan (eds.), *Proceedings of the Conference on Natural Resources And Life Sciences 2022 (NRLS-BIO 2022)*, Advances in Biological Sciences Research 38,
https://doi.org/10.2991/978-94-6463-322-1_19

be used in QSAR modeling. These compounds were built in 1D and 2D, and their activity value was converted to pIC50. On the other hand, ADMET prediction was performed using the full data set.

2.2. LFER Hansch QSAR Model

LFER Hansch equation was built using DTC-QSAR software (available from https://dtclab.webs.com/software-tools). Three types of descriptors were generated in this study (lipophilic, steric, electronic) as independent variables. LogP and $(LogP)^2$ as lipophilic descriptors were calculated using the pkCSM web server [14]. Molecular weight and solvent-accessible surface area (SASA) as steric descriptors were calculated using MarvinSketch 22.5 (available from https://chemaxon.com). EHOMO, ELUMO, and ETOT as electronic descriptors were calculated using MOPAC2016 [15] (available from https://openmopac.net/MOPAC2016.html), where 3D structures were generated using PM6 basis set [16]. Before the QSAR model building, the dataset was split into a training set and a test set with a ratio of 4:1 using the Kennard-Stones algorithm [17]. Various statistical parameter was used to evaluate the quality and validity of the QSAR model, such as $R^2 > 0,7$; Q^2 LOO > 0,6; R^2-Q^2 LOO < 0,1; $\underline{R_m^2} > 0,65$; $\Delta R_m^2 < 0,2$; Q^2F1, $Q^2F2 > 0,7$; and CCC > 0,85 [18].

2.3. 3D QSAR Model

A three-dimensional QSAR model was built using the webserver Cloud-3D QSAR [19]. Compounds in the dataset were prepared in a 1D format to be submitted to the web server. Similar to the Hansch model, a dataset was split similarly to validate the result. The 3D QSAR model is visualized as a contour map with specific colors indicating the most prominent effect in the particular region. Steric group addition is guided by green and yellow, where the former indicates a positive effect on activity, while the latter indicates otherwise. Electronic effects are denoted with red and blue, where the former indicates the desirable addition of the negatively charged group, while the latter indicates the desirable addition of the positively charged group [19,20].

2.4. ADMET Prediction

ADME parameters of 60 febrifugine derivatives were predicted using the pkCSM web server [14]. These parameters were human intestinal absorption (HIA), the volume of distribution at steady state condition (VDSS), various cytochrome-P450 related interactions, and total clearance value. In addition, toxicity prediction was performed using ProTox-II [21]. This web server yields predicted toxicity value in LD50, which is then classified into six classes of oral toxicity.

3. RESULTS & DISCUSSION

Quantitative Structure-Activity Relationships (QSAR) is one of the approaches which can be implemented to explore the correlation between chemical structures and their bioactivity [22]. LFER Hansch is among the earliest method, founded by the postulate that the bioactivity of a compound is influenced by lipophilic, steric, and electronic aspects [23]. This method created a mathematical model between various febrifugine analogs and their antimalarial activity. The result showed that the second order of LogP plays an important role in defining the structure-activity correlation. According to McFarland's hypothesis, nonlinear interaction between LogP and activity is likely to be observed since a molecule must pass the phospholipid bilayer membrane before interacting with the target receptor [24]. However, this current model is limited in its applicability domain from the dataset of febrifugine analogs with a pIC50 value of more than 5.

$$pIC50 = 0,069(\pm 0,0009)\,(logP)^2 + 3,5234(\pm 0,0461) \quad (1)$$

($n = 40$ $R^2 = 0.9938$ Q^2 LOO $= 0.9926$ R_m^2 average $= 0.9895$ R^2-Q^2 LOO $= 0.0012$ $\Delta R_m^2 = 0.0037$ Q^2 F1 $= 0.9956$ Q^2 F2 $= 0.9955$ CCC $= 0.9978$)

3D-QSAR is a QSAR model that correlates various molecules' three-dimensional structures with their biological activity. This method uses an atom-based descriptor derived from the spatial representation of molecules [20]. Here, the 3D QSAR model was formulated using web server Cloud-3D QSAR, which uses the CoMFA approach and partial-least square for statistical evaluation. The resulting model should correspond with statistical parameters such as R^2, Q^2, and R^2_{pred} [25]. Our best model complies with the parameters ($R^2 = 0.9393$ $Q^2 = 0.6098$) but with a poor R^2_{pred} value ($R^2_{pred} = -1.3418$) which indicated low predictability. The contour map showed that steric functional group addition is necessary for C6 and 7 of quinazolinone and C4 and 5 of piperidine. Meanwhile, further improvement could be expected by adding a negatively charged functional group in C5 of quinazolinone.

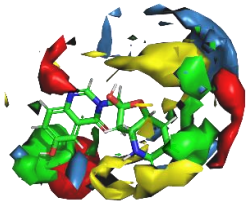

Figure 1 3D QSAR contour map of febrifugine and their analogs

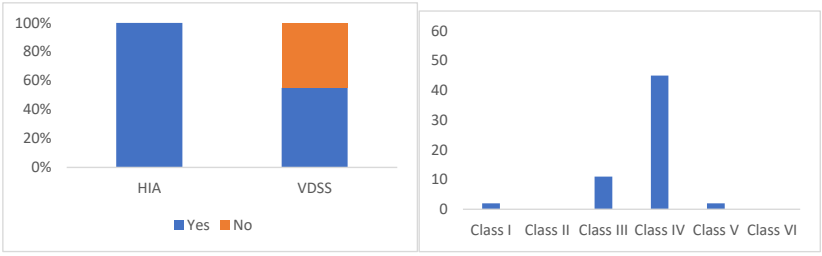

Figure 2 Prediction of absorption, distribution (left), and oral toxicity class (right) of 60 febrifugine analogs

Table 1. Febrifugine analogs dataset used in QSAR model building

Reference	Compound	IC50 (μM)
[9]	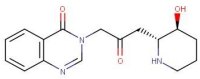	7.0×10^{-4}
[9]	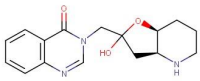	3.4×10^{-3}
[9]	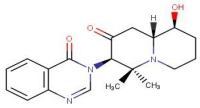	1.6×10^{-3}
[9]	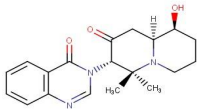	2.8×10^{-3}
[10]	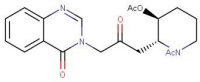	9.1×10^{-1}
[10]	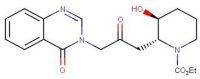	4.8
[10]	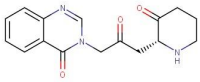	2.0×10^{-2}
[10]	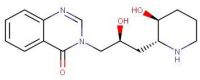	2.0×10^{-2}
[10]	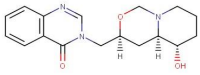	3.7×10^{-3}
[10]	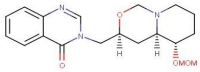	8.6×10^{-3}

Reference	Compound	IC50 (μM)
[10]	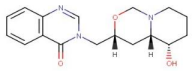	8.4×10^{-1}
[10]	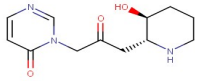	6.0×10^{-1}
[10]	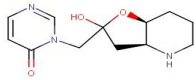	4.0×10^{-2}
[10]	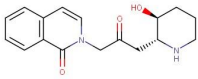	5.0×10^{-1}
[10]	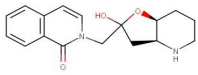	2.1
[10]	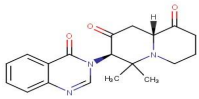	1.9×10^{-3}
[10]	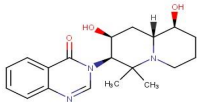	4.0×10^{-1}
[10]	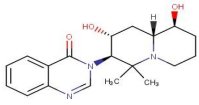	3.0×10^{-1}
[10]	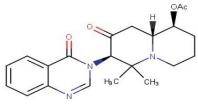	3.6×10^{-3}

Reference	Compound	IC50 (μM)
[10]	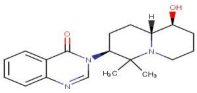	8.3×10^{-1}
[10]	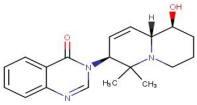	4.8
[10]	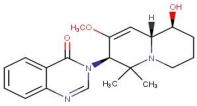	1.3
[10]	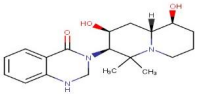	4.2×10^{-1}
[10]	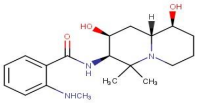	6.0×10^{-1}
[10]	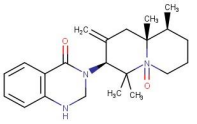	1.0×10^{-1}
[10]	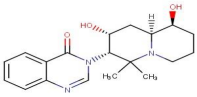	8.0×10^{-1}
[10]	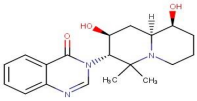	3.4
[11]	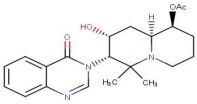	4.0×10^{-1}
[11]	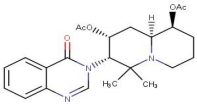	7.0
[11]	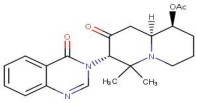	1.9×10^{-2}

Reference	Compound	IC50 (μM)
[12]	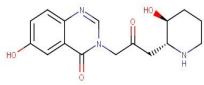	2.2×10^{-3}
[12]	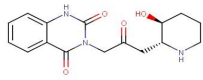	6.6
[12]	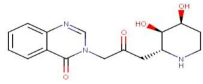	2.2×10^{-2}
[12]	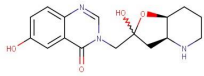	2.7×10^{-4}
[12]	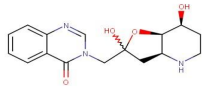	1.5×10^{-1}
[13]	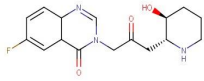	2.3×10^{-3}
[13]	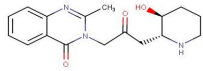	0.36
[13]	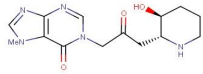	1.66
[13]	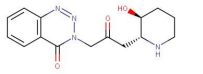	0.51
[13]	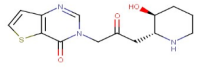	9.95×10^{-3}
[13]	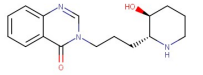	0.0783
[14]	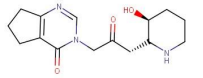	0.256
[14]	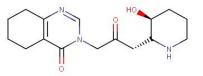	0.258
[14]	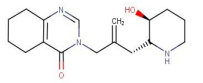	0.128
[14]	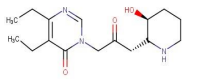	0.640

Reference	Compound	IC50 (µM)
[14]	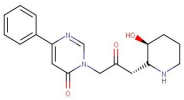	0.286
[14]	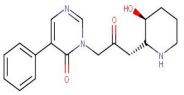	0.128
[14]	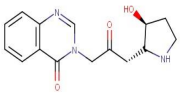	2.126
[14]	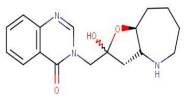	0.390
[14]	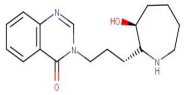	1.808

In silico predictions were performed to assess the profile of ADMET parameters of febrifugine analogs. Generally, all febrifugine analogs possess acceptable absorption and distribution, which is indicated by an HIA value of more than 30% [26] and a VDSS value of more than 0.45 [27], respectively. Cytochrome P450 interaction prediction yielded 11 compounds as 3A4 substrates, 8 as 1A2 inhibitors, and one as 2C19 inhibitors. The average value of log total clearance from 60 compounds is 0.971 (ml/min/kg). This value represents the rate of hepatic and renal excretion of a compound, where a high value indicates a faster excretion process. Ultimately, LD50 analysis of febrifugin analogs showed that most of the compound is classified in GHS Class IV for acute oral toxicity [26].

4. CONCLUSION

We have developed LFER Hansch and 3D-QSAR models for febrifugine derivates against *P. falciparum* strain FCR-3. It is argued that $(LogP)^2$ is important in improving antimalarial activity. In addition, substituting the steric functional group in the quinazolinone and piperidine ring of febrifugine could improve their bioactivity. However, further dataset and method selection are still needed to validate the 3D-QSAR model.

AUTHORS' CONTRIBUTIONS

Tegar Achsendo Yuniarta and Dini Kesuma conceptualized the study, Nur Aina performed data collection, Nur Aina and Tegar Achsendo Yuniarta performed data analysis, Nur Aina and Tegar Achsendo Yuniarta wrote the manuscript, all authors have read and agreed with the manuscript.

ACKNOWLEDGMENTS

The authors would like to thank the NRLS committee for the opportunity to present this study and receive valuable insights and feedbacks.

REFERENCES

[1] R.B. McFee, Malaria (Plasmodium), Disease-a-Month, 2013, 59(12), 441-442.

[2] World Health Organization, World Malaria Report, World Health Organization, 2021.

[3] O. Müller, G.Y. Lu, L.v. Seidlein, Geographic expansion of artemisinin resistance, Journal of Travel Medicine, 2019, 26(4) (2019) taz030. doi: 10.1093/jtm/taz030.

[4] S. Smullen, N.P. McLaughlin, P. Evans, Chemical synthesis of febrifugine and analogues, Bioorganic & Medicinal Chemistry, 2018, 26(9), 2199-2220. doi: 10.1016/j.bmc.2018.04.027.

[5] S. Jiang, Q. Zeng, M. Gettayacamin, A. Tungtaeng, S. Wannaying, A. Lim, P. Hansukjariya, C.O. Okunji, S. Zhu, D. Fang, Antimalarial Activities and Therapeutic Properties of Febrifugine Analogs, Antimicrobial Agents and Chemotherapy, 2005, 49(3) 1169-1176. doi: 10.1128/AAC.49.3.1169-1176.2005.

[6] T.L. Keller, D. Zocco, M.S. Sundrud, M. Hendrick, M. Edenius, J. Yum, Y-J. Kim, H-K. Lee, J.F. Cortese, D.F. Wirth, J.D. Dignam, A. Rao, C-Y. Yeo, R. Mazitschek, M. Whitman, Halofuginone and other febrifugine derivatives inhibit prolyl-tRNA synthetase, Nature Chemical Biology 8,2012, 311-317. doi: 10.1038/nchembio.790.

[7] V. Jain, M. Yogavel, Y. Oshima, H. Kikuchi, B. Touquet, M-A. Hakimi, A. Sharma, Structure of Prolyl-tRNA Synthetase-Halofuginone Complex Provides Basis for Development of Drugs against Malaria and Toxoplasmosis, Structure, 2015), 23(5), 819-829. doi: 10.1016/j.str.2015.02.011.

[8] H. Zhou, L. Sun, X-L. Yang, P. Schimmel, ATP-directed capture of bioactive herbal-based medicine on human tRNA synthetase, Nature, 2013, 494 , 121-124.doi: 10.1038/nature11774.

[9] Y. Takaya, H. Tasaka, T. Chiba, K. Uwai, M. Tanitsu, H-S. Kim, Y. Wataya, M. Miura, M. Takeshita, Y. Oshima, New Type of Febrifugine Analogues, Bearing a Quinolizidine Moiety, Show Potent Antimalarial Activity against *Plasmodium* Malaria Parasite, Journal of Medicinal Chemistry, 1999, 42, 3163-3166. doi: 10.1021/jm990131e.

[10] H. Kikuchi, H. Tasaka, S. Hirai, Y. Takaya, Y. Iwabuchi, H. Ooi, S. Hatakeyama, H-S. Kim, Y. Wataya, Y. Oshima, Potent Antimalarial Febrifugine Analogues against the *Plasmodium* Malaria Parasite, Journal of Medicinal Chemistry, 2002, 45(12), 2563-2570. doi: 10.1021/jm010448q..

[11] S. Hirai, H. Kikuchi, H-S. Kim, K. Begum, Y. Wataya, H. Tasaka, Y. Miyazawa, K. Yamamoto, Y. Oshima, Metabolites of Febrifugine and Its Synthetic Analogue by Mouse Liver S9 and Their Antimalarial Activity against *Plasmodium* Malaria Parasite, Journal of Medicinal Chemistry, 2003, 46(20), 4351-4359. doi: 10.1021/jm0302086.

[12] H. Kikuchi, K. Yamamoto, S. Horoiwa, S. Hirai, R. Kasahara, N. Hariguchi, M. Matsumoto, Y. Oshima, Exploration of a New Type of Antimalarial Compounds Based on Febrifugine, Journal of Medicinal Chemistry, 2006,49(15), 4698-4706. doi: 10.1021/jm0601809.

[13] H. Kikuchi, S. Horoiwa, R. Kasahara, N. Hariguchi, M. Matsumoto, Y. Oshima, Synthesis of febrifugine derivatives and development of an effective and safe tetrahydroquinazoline-type antimalarial, European Journal of Medicinal Chemistry, 2014, 76, 10-19. doi: 10.1016/j.ejmech.2014.01.036.

[14] D.E.V. Pires, T.L. Blundell, D.B. Ascher, pkCSM: Predicting Small-Molecule Pharmacokinetic and Toxicity Properties Using Graph-Based Signatures, Journal.of Medicinal Chemistry, 2015, 58(9), 4066-4072. doi: 10.1021/acs.jmedchem.5b00104.

[15] J.J.P. S, tewart, MOPAC: A semiempirical molecular orbital program, Journal of Computer-Aided Molecular Design, 1990, 4 , 1-103. doi: 10.1007/BF00128336.

[16] J.J.P. Stewart, Optimization of parameters for semiempirical methods V: Modification of NDDO approximations and application to 70 elements, Journal of Molecular Modeling, 2007, 13, 1173-1213. doi: 10.1007/s00894-007-0233-4.

[17] T.M. Martin, P. Harten, D.M. Young, E.N. Muratov, A. Golbraikh, H. Zhu, A. Tropsha, Does Rational Selection of Training and Test Sets Improve the Outcome of QSAR Modeling?, Journal of Chemical Information and Modelling, 2012, 52(10) 2570-2578, doi: 10.1021/ci300338w.

[18] I.G.A. Sumartha, T.A. Yuniarta, D. Kesuma, QSAR Study Of Pyrazole-Urea Hybrid Compounds As Antimalarial Agent Via Prolyl-tRNA Synthetase Inhibition, Rasayan Journal of Chemistry, 2022, 15(2), 1450-1460. doi: 10.31788/RJC.2022.1526811

[19] Y-L. Wang, F. Wang, X-X. Shi, C-Y. Jia, F-X. Wu, G-F. Hao, G-F. Yang, Cloud 3D-QSAR: a web tool for the development of quantitative structure–activity relationship models in drug discovery, Briefings in Bioinformatics, 2021, 22(4). doi: 10.1093/bib/bbaa276.

[20] J. Verma, V.M. Khedkar, E.C. Coutinho, 3D-QSAR in Drug Design - A Review, Current Topics in Medicinal Chemistry, 2010, 10(1), 95-115. doi: 10.2174/156802610790232260.

[21] P. Banerjee, A.O. Eckert, A.K. Schrey, R. Preissner, ProTox-II: a webserver for the prediction of toxicity of chemicals, Nucleic Acid Research, 2018, 46(W1), W257-W263. doi: 10.1093/nar/gky318.

[22] K. Roy, S. Kar, R.N. Das, A Primer on QSAR/QSPR Modeling: Fundamental Concepts, Springer, 2015

[23] C. Hansch, The advent and evolution of QSAR at Pomona College, Journal of Computer-Aided Molecular Design, 2011, 25,495-507. doi: 10.1007/s10822-011-9444-y.

[24] J.W. McFarland, Parabolic relation between drug potency and hydrophobicity, Journal of Medicinal Chemistry,1970, 13(6), 92-1196. doi: 10.1021/jm00300a040.

[25] P. Nunthanavanit, N.G. Anthony, B.F. Johnston, S.P. Mackay, J. Ungwitayatorn, Archiv der Pharmazie-Chemistry in Life Science 341 (2008) 357-364.

[26] United Nations, GloballyHarmonized SystemOf Classification And LabellingOf Chemicals (GHS), United Nations, 2011.